IOP Publishing Journal of Physics: Condensed Matter
J. Phys.: Condens. Matter **32** (2020) 275001 (6pp) https://doi.org/10.1088/1361-648X/ab7e59

# Magnetism manipulation of $Co_n$-adsorbed monolayer $WS_2$ through charge injection

**Weiqing Tang[1], Congming Ke[1], Kai Chen[1], Zhiming Wu[1,4], Yaping Wu[1,2,3,4], Xu Li[1] and Junyong Kang[1]**

[1] Department of Physics, OSED, Fujian Provincial Key Laboratory of Semiconductor Materials and Applications, Xiamen University, Xiamen, 361005, People's Republic of China
[2] National Laboratory of Solid State Microstructures, Nanjing University, Nanjing 210093, People's Republic of China
[3] Fujian Provincial Key Laboratory of Quantum Manipulation and New Energy Materials, People's Republic of China

E-mail: zmwu@xmu.edu.cn and ypwu@xmu.edu.cn

Received 18 January 2020, revised 19 February 2020
Accepted for publication 10 March 2020
Published 9 April 2020

**Abstract**

The design and manipulation of magnetism in low-dimensional systems are desirable for the development of spin electronic devices. Here, we design two kinds of Co-adsorbed monolayer $WS_2$ frameworks, i.e. $Co_1/WS_2$ and $Co_2/WS_2$, and comprehensively explore the dependences of their magnetic properties on injected charge by using first-principles calculations. The value of magnetic moment can be tuned almost linearly through injecting charge due to the modulated interaction and charge transferring between Co atom and monolayer $WS_2$. A transition from ferromagnetism to non-ferromagnetism occurs in $Co_1/WS_2$ system when 1 e/unit cell charge is injected. Furthermore, the magnetic anisotropy can be manipulated by injecting charge as well. The magnetic anisotropy energy (MAE) in $Co_1/WS_2$ system sharply increases from −4.16 to 2.47 (0.99) meV when injected charge vary from 0.0 to 0.2 (−0.2) e/unit cell, meaning a transition of the magnetic easy axis from in-plane to out-of-plane direction. Similarly, in $Co_2/WS_2$ system, the magnetic easy axis also can be modified to out-of-plane direction through injecting 0.1 e/unit cell charge. It is found that the changes of Co-3d states are responsible for the tunable magnetic anisotropy. This work provides a theoretical understanding on effective manipulation of magnetism in low-dimensional system.

Keywords: magnetic anisotropy, magnetic moment, charge injection, 2D materials

(Some figures may appear in colour only in the online journal)

## 1. Introduction

Spintronics is an interactive combination of electronics and magnetics that has been growing fast over the past decades due to its great potential for the applications of low power-consumed and novel functional devices [1–6]. Two dimensional (2D) transition-metal dichalcogenides (TMD), such as $WS_2$ and $MoS_2$, possess novel spin- and valley-coupled physical properties owing to the strong spin–orbit coupling (SOC), and have been extensively studied [7, 8]. Transition metals have strong spin interaction with TMD materials [9–12]. Considering the high polarizability of ferromagnetic materials (FMs), FM/TMD nanostructures have often been constructed especially for the applications in magnetic tunnel junctions and magnetic memory [13–15]. The control of their magnetic properties is crucial for the device performance. For instance, the perpendicular magnetic anisotropy (PMA) with magnetic easy axis perpendicular to the surface is beneficial for the improvement of the storage density of magnetic memory [16, 17]. A record-high magnetic anisotropy energy (MAE) of ∼60 meV was achieved in individual Co atom/MgO heterojunctions owing to the orbital multiplet effect of the high-spin Co atom in their special tetragonal ligand field [18, 19]. Actually, a strong magnetic anisotropy can also be generated in 3D transition metal/TMD system through proximity effect. It is

[4] Author to whom any correspondence should be addressed.

 

reported that Fe and Co atoms on the W vacancy of monolayer $WS_2$ can achieve the giant MAE of 29 and 34 meV, respectively [20]. In experiment, monomers and dimers of Co atoms have been successfully deposited on 2D materials by electron-beam evaporator at ultralow temperature [21, 22]. In addition, the manipulation of the magnetic anisotropy is generally necessary to functionalize magnetic devices. Currently, applying a magnetic field or injecting spin current is popular to manipulate magnetic anisotropy [23, 24]. As a convenient and uncontaminated method, charge injection can greatly change the MAE in a certain system [25], such as Fe/graphene and Fe/$MoS_2$ bilayer systems [26, 27], showing a great potential for the control of magnetic anisotropy. Up to date, the design and manipulation of magnetism in a low-dimensional structure are still challenging for the development of spintronics.

In this work, we construct two kinds of Co-adsorbed monolayer $WS_2$ frameworks, $Co_1/WS_2$ and $Co_2/WS_2$, and comprehensively investigate the dependences of magnetic properties, especially magnetic moment and MAE, on injected charge based on first-principles calculations. Their stable structures are identified by the calculated binding energies. The changes of magnetic properties in the two systems are analyzed by employing total density of states (TDOS). Furthermore, the physical mechanism of the modulated magnetic moment in the systems are clarified through the simulation of spin charge densities and differential charge densities, and meanwhile, MAE origination is analyzed by orbital decomposed densities of Co-3d states.

## 2. Calculation details

The first-principles calculations of pristine and Co-adsorbed monolayer $WS_2$ are performed by using the spin-polarized periodic density functional theory (DFT), as implemented in Vienna *ab initio* simulation package (VASP) code with the projector augmented wave (PAW) pseudopotential [28–30]. A $4 \times 4$ supercell and a vacuum region with a height of 25 Å are set to eliminate the interlayer interaction and the interaction between Co atoms. The exchange-correlation effects are treated by Perdew–Burke–Ernzerh of generalized gradient approximation (GGA-PBE) [31]. The two dimensional Brillouin zone (BZ) is sampled with a $9 \times 9 \times 1$ Monkhorst–Pack grid of $k$ points, and a cutoff energy of 364 eV is used for the plane wave basis set. All the structures are fully relaxed until the Hellmann–Feynman forces and the total energy are less than 0.01 eV $Å^{-1}$ and $10^{-6}$ eV, respectively. The MAE is calculated through the energy difference when the magnetization directions are in the $xy$ plane ($E_{ll}$) and along the $z$ axis ($E_{\perp}$), MAE $= E_{ll} - E_{\perp}$, as the SOC is performed [32–34]. To accurately estimate the MAE, the energy cutoff and $k$-points are optimized in our calculations.

## 3. Results and discussion

Geometric configuration of the pristine monolayer $WS_2$ is exhibited in figure 1(a). W and S atoms alternately bond and form an ideal hexagonal honeycomb structure in the planar projection, which is similar to that of other 2D TMD materials

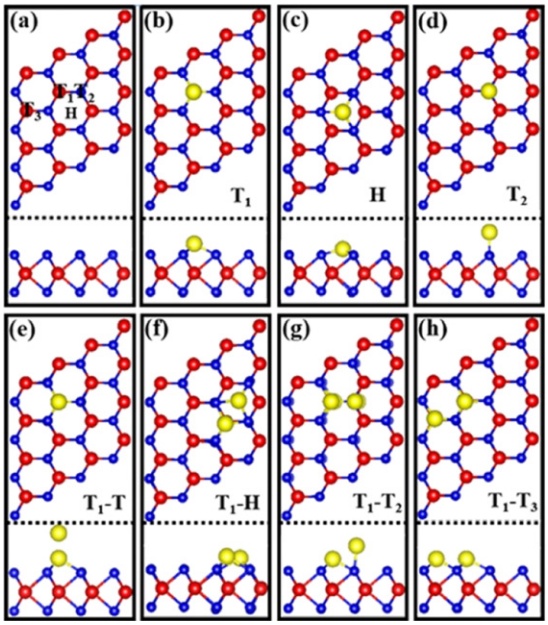


**Figure 1.** Top and side view of (a) $WS_2$ monolayer, $Co_1/WS_2$ system with a Co adatom locating at $T_1$ (b), H (c) and $T_2$ (d) site of $WS_2$ surface, and $Co_2/WS_2$ system with the second Co adatom locating at T (e), H (f), $T_2$ (g) and $T_3$ (h) site of $WS_2$ surface. Red, blue and yellow spheres represent W, S and Co atoms, respectively.

[35]. The optimized thickness and lattice constant of monolayer $WS_2$ are 4.47 Å and 3.19 Å, respectively; the length of W–S bond and the angle of S–W–S bond are measured to be 2.42 Å and 81°, respectively, which are well consistent with previous work [36]. Considering the geometric symmetry of $WS_2$ surface, three high symmetrical sites, i.e. the top site of W atom ($T_1$ or $T_3$), hollow site (H), and the top site of S atom ($T_2$), are selected as the adsorption sites, as shown in figures 1(b)–(d). To evaluate the stability of structures, the adsorption energies are calculated through the equation $E_{ad} = E_{WS_2} + nE_{Co} - E_{nCo/ws_2}$, where $E_{WS_2}$, $E_{Co}$, and $E_{nCo/ws_2}$ denote the energies of the pristine $WS_2$, Co atom, and $Co_n/WS_2$ system, respectively; $n$ is the number of Co adatoms. The calculated adsorption energies of single Co adatom on $T_1$ site, H site and $T_2$ site are 3.2 eV, 2.55 eV, and 1.14 eV, respectively. The configuration with the Co adatom on $T_1$ site has the largest adsorption energy, meaning that the top site of W atom is the most stable adsorption site for single Co adatom. As for the $Co_2/WS_2$ system, considering the geometric symmetry, the second Co adatom most probably locates on the top site of the first Co adatom, or the H, $T_2$, and $T_3$ sites nearest the first Co adatom, as shown in figures 1(e)–(h). The calculated adsorption energies are 5.30 eV, 5.70 eV, 5.46 eV, and 6.27 eV, respectively, when ferromagnetic interaction exists in two Co atoms. Obviously, the $Co_2/WS_2$ system with Co adatoms locating at $T_1$ and $T_3$ sites, as shown in figure 1(h), has the largest adsorption energy, indicating the most stable configuration. Meanwhile, the adsorption energy of antiferromagnetic Co atoms on the top of W sites is also calculated, the value (6.11 eV) is smaller than that of ferromagnetic state. Therefore, the two most stable configurations are adopted in the following investigation.

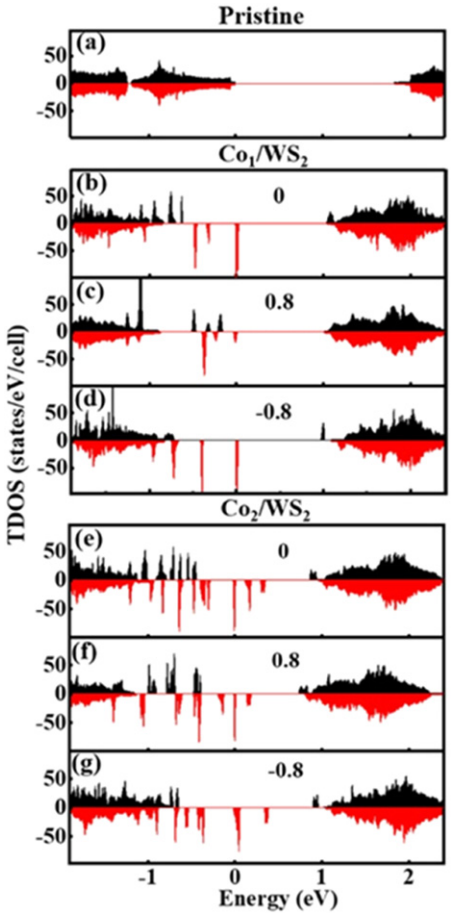


**Figure 2.** TDOS of (a) pristine $WS_2$ monolayer and $Co_{(1,2)}/WS_2$ systems under the different injected charges, (b) and (e) 0 e/unit, (c) and (f) 0.8 e/unit, (d) and (g) −0.8 e/unit.

To reveal the effect of Co adatoms on the electronic and magnetic properties of monolayer $WS_2$, TDOS is plotted in figure 2. As shown in figure 2(a), the TDOS of pristine $WS_2$ exhibits a coincident distribution in spin-up and spin-down channels, indicating a non-magnetic ground state. The band gap is measured as 1.82 eV, slightly larger than that of bulk material due to the absence of van der Waals (vdW) interlayer interaction in monolayer $WS_2$. For the $Co_1/WS_2$ system, as shown in figure 2(b), the adsorption of the Co atom results in the upshift of Fermi energy level ($E_f$) toward the conduction band minimum (CBM), indicating an n-type doping effect. Meanwhile, three impurity states originating from the Co atom appear in the gap (figure 2(b)) and result in the uncoincident TDOS around the $E_f$, demonstrating the magnetic system of $Co_1/WS_2$. Furthermore, the impurity states near the $E_f$ contribute only to the spin-down channel, implying the half-metallic feature. In this sense, this system is expected to provide 100% spin-polarized current. As for the $Co_2/WS_2$ system, as shown in figure 2(e), the TDOS is similar to that of $Co_1/WS_2$ system, and the main difference is that more impurity states appear in the spin-down channels. This demonstrates that the $Co_2/WS_2$ system has the stronger coupling interaction than the $Co_1/WS_2$ system.

To modify the magnetic properties of the two kinds of configurations, charge injection is further employed. As shown in figure 2(c), when 0.8 e/unit cell charge is injected to the $Co_1/WS_2$ system, the spin-up impurity states upshift to the upper energy and tend to form a coincident distribution with spin-down impurity states; in addition, the intensities of both spin-up and spin-down impurity states distinctly decay. As injecting −0.8 e/unit cell charge, the spin-up impurity states move to the deeper energy level and their intensities prominently decrease. By contrast, the intensity of spin-down impurity states increase compared with that without injected charge (figure 2(d)), and the difference in energy level for the three impurity states becomes large. As for the $Co_2/WS_2$ system, the variation tendency of $E_f$ for the spin-up and spin-down channels is similar to that of $Co_1/WS_2$ system when the addition charge is injected.

To comprehensively explore the modulated effect of injected charge on magnetic properties of $Co_n/WS_2$ systems, the dependences of total energy, spin polarization energy, magnetic moment and MAE on injected charge are plotted in figure 3. As shown in figure 3(a), their total energies in both the systems continuously increase with the increase of the injected positive charge due to the enhanced chemical potential [30]. In addition, their spin polarized energies, defined as the difference between the energy with and without the spin polarization, decrease with the increase of the injected positive charge, indicating the unstable spin-states (figure 3(b)). As a result, the values of magnetic moment almost linearly decrease for both the systems (figure 3(c)). Notably, the magnetic moment of the $Co_1/WS_2$ system drops to 0 $\mu_B$ under 1 e/unit cell injected charge, demonstrating a transition from ferromagnetic system to non-ferromagnetic system. Excitingly, the MAE of two systems can be effectively modulated by charge injection as well, as shown in figure 3(d). For both the pristine system, they have negative MAE value, indicating the in-plane magnetization easy axis. However, the changed tendencies of magnetization easy axis with injected charge are different for the two systems. For the $Co_1/WS_2$ system, the MAE value sharply increases from −4.16 to 2.47 (0.99) meV when injected charge vary from 0.0 to 0.2 (−0.2) e/unit cell, meaning a transition in the magnetization axis from in-plane direction to out-of-plane direction. As for the $Co_2/WS_2$ system, the magnetization easy axis changes from in-plane direction to out-of-plane direction with the increased injected positive charge. However, the MAE value always keeps a negative value when different negative charge is injected, meaning an unchanged magnetization easy axis. In addition, the MAE of cobalt layer absorbed monolayer $WS_2$ and a sandwich structure ($WS_2$–Co–$WS_2$) are calculated, and their values are −0.55 and –0.32 meV, respectively, implying that their magnetic easy axis is parallel to in-plane direction.

The spin charge densities of the two systems without and with the injected charge are further calculated to comprehend the origination of the changes of magnetic properties. As shown in figure 4, spin charges are mainly contributed by the adsorbed Co atoms and the nearest-neighbor W and S atoms. For $Co_1/WS_2$ system, spin-up charge densities mainly distribute around the Co atom and the nearest-neighbor W

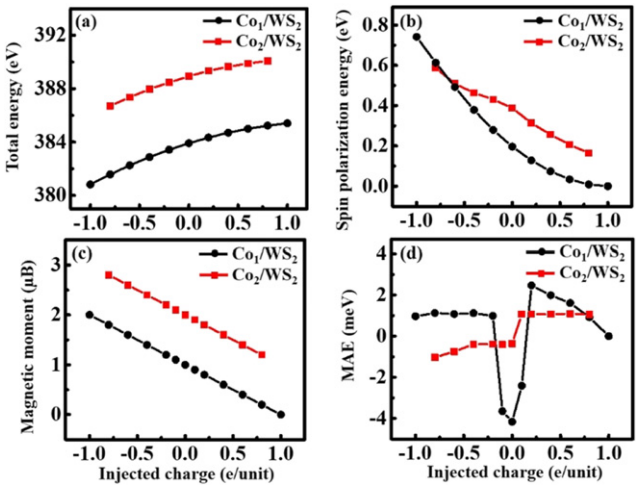


**Figure 3.** The dependences of (a) the total energy, (b) spin polarization energy, (c) magnetic moment, and (d) MAE on injected charge in $Co_{(1,2)}/WS_2$ systems.

atom, and the spin-down charge densities locate around the three nearest-neighbor S atoms, indicating an antiferromagnetic coupling between the Co atom and the S atoms. In the case of the pristine $Co_1/WS_2$ system, the spin-up density is obviously greater than the spin-down one, resulting in the appearance of magnetism in the system. When the 0.8 e/unit cell charge is injected, both the spin-up and the spin-down densities substantially reduce, leading to the decrease of total magnetic moments (as shown in figure 3(c)). However, when the −0.8 e/unit cell charge is injected, as shown in figure 4(c), the spin-up densities dramatically increase, whereas the spin-down densities almost keep constant, resulting in the increase of magnetic moments. Different from the $Co_1/WS_2$ system, spin-down charge densities mainly distribute around the W atoms in the beneath of Co adatoms, and a small number of spin-up densities are induced in the nearest-neighbor S atoms for the pristine $Co_2/WS_2$ system. With the injection of 0.8 e/unit cell charge, the spin-up charge densities originating from two Co adatoms become weak, whereas the spin-down densities slightly increase, which contributed to the reduction of magnetic moment (figure 3(c)). However, with the injection of −0.8 e/unit cell charge, not only the spin-up charge densities around the two Co adatoms increase, but also the spin states around W atoms even transform from the spin-down to the spin-up (see figure 4(f)). Both the behaviors contribute to the increase of the total magnetic moments in this system.

Essentially, the changes of their magnetic properties are attributed to the bond interaction and charge redistribution. Hence, the differential charge densities are further calculated to reveal the physics mechanism of the changing magnetic moment in the two systems. For both the pristine systems, as shown in figures 5(a) and (b), negative charge densities are observed around the S and Co atoms, while positive charge densities are observed in the middle of the Co–S bonds, implying the covalent interaction of Co–S bonds. With the injection of 0.8 e/unit cell charge, as shown in figures 5(c) and (d), more electrons accumulate in the Co–S bond for both the

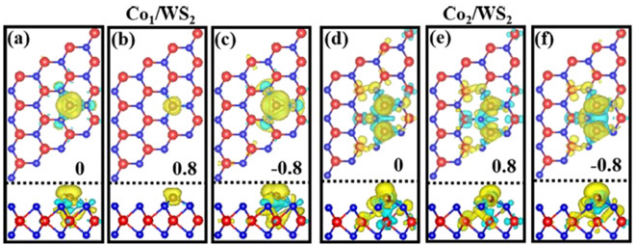


**Figure 4.** Spin charge densities of (a)–(c) $Co_1/WS_2$ system and (d)–(f) $Co_2/WS_2$ system under different injected charge. The yellow and blue colors denote the positive spin charge densities and negative spin charge densities, respectively. The isosurface of the spin charge densities is set to 0.02 e $Å^{-3}$.

systems, resulting in the stronger bond interaction between the Co and S atoms. The charge transfer results in the decreased unpaired electrons of Co atoms, and thus the reduced magnetic moment in the systems [37]. When −0.8 e/unit cell charge is injected, as shown in figures 5(e) and (f), all the above evolution tendencies reverse. The unpaired electrons increase and bond interaction becomes weak, resulting in the increase of the total magnetic moment of the system shown in figure 3(c).

In order to obtain a fundamental understanding of the changed magnetic anisotropy, we calculated the orbital-decomposed densities of Co-3d states under different injected charge, as shown in figure 6. According to the second-order perturbation theory [38], the MAE arising from the SOC interaction can be approximately formulated as

$$\mathrm{MAE} = E_{\parallel} - E_{\perp} \approx \xi^2 \sum_{\mu,\sigma} \frac{\mu^m |L_z| \sigma^{n2} - \mu^m |L_x| \sigma^{n2}}{E_\mu - E_\sigma}$$

where $\mu^m$ ($\sigma^n$) and $E_\mu$ ($E_\sigma$) denote the eigenstates and eigenvalues of the occupied (unoccupied) states in spin state $m$ ($n$); $\xi$ is the strength of SOC. In more detail, for $mn = \uparrow\uparrow$ or $\downarrow\downarrow$, positive (negative) contribution to MAE is determined by the matrix elements of angular momentum operators $L_z(L_x)$ across the unoccupied and occupied states, while for $mn = \uparrow\downarrow$, positive (negative) contribution arises from the $L_x(L_z)$ operators. This equation implies that the localized impurity states of Co adatoms around $E_f$ are mainly contributed to the calculated unquenchable orbital moments [39]. Hence, the orbital-decomposed DOS at turning points of MAE are considered. As shown in figure 6, in both the systems, the nonvanishing angular momentum matrix elements between d states comprise of $\langle xz|L_z|yz\rangle$, $\langle x^2 - y^2|L_x|yz, xz\rangle$, $\langle xy|L_x|yz, xz\rangle$, and $\langle z^2|L_x|yz, xz\rangle$ (bra and ket can be exchanged), and only the states of $mn = \downarrow\downarrow$ make contributions to the MAE because of no spin-up states around $E_f$. As for pristine $Co_1/WS_2$ configuration, there are large unoccupied $d_{yz}/d_{xz}$ minority-spin states as well as the occupied $d_{xy}/d_{x^2-y^2}$ minority-spin states around $E_f$ (seeing figure 6(a)), resulting in the large value of $\langle xy|L_x|yz, xz\rangle$ and $\langle x^2 - y^2|L_x|yz, xz\rangle$, which makes the considerable contribution to the negative MAE. As injecting 0.2 e/unit charge, the spin-conservation term $\langle xz|L_z|yz\rangle$ and $\langle yz|L_z|xz\rangle$ with the positive contribution to MAE increase because of the dramatical enhancement of the occupied $d_{yz}/d_{xz}$ minority-spin states

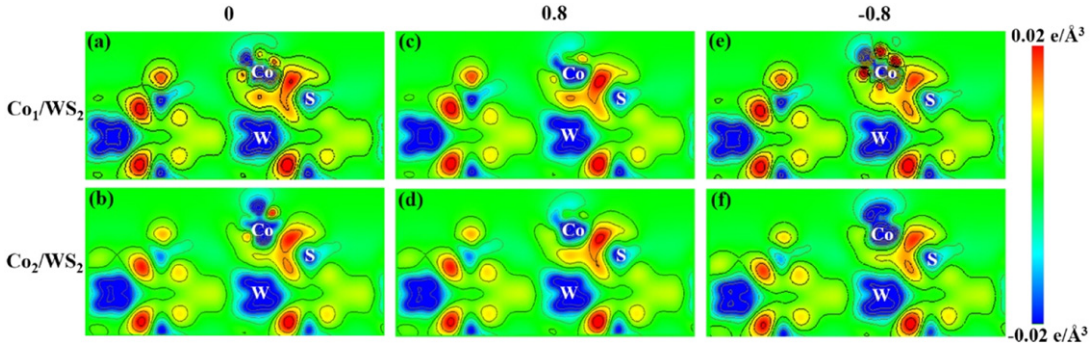


**Figure 5.** Differential charge densities of the two systems under different injected charge, (a) and (b) 0 e/unit, (c) and (d) 0.8 e/unit, (e) and (f) −0.8 e/unit.

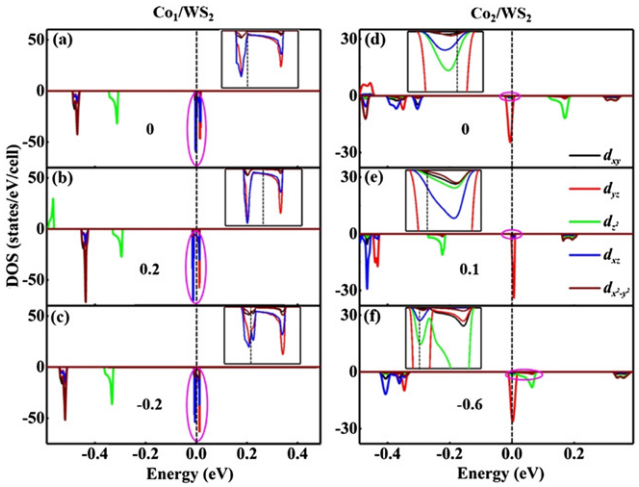


**Figure 6.** 3d-orbital decomposed DOS of Co atom for the two systems under different injected charge, (a) 0 e/unit, (b) 0.2 e/unit, (c) −0.2 e/unit, (d) 0 e/unit, (e) 0.1 e/unit, (f) −0.6 e/unit.

and unoccupied $d_{yz}$ minority-spin states (seeing figure 6(b)). Consequently, the MAE value increases from −4.16 to 2.47 meV (seeing figure 3(d)). When injecting −0.2 e/unit charge, the $E_f$ slightly moves toward the lower energy, resulting in the dramatical decrease of the occupied $d_{xy}/d_{x^2-y^2}$ minority-spin states, and thus spin-conservation term $\langle x^2-y^2, xy|L_x|xz\rangle$ becomes a small value. Meanwhile, the sharp augment of the unoccupied spin-down $d_{yz}$ states leads to the increase of $\langle xz|L_z|yz\rangle$. Hence, the MAE turns to a positive value of 0.99 meV in contrast to that of pristine $Co_1/WS_2$ system. As for the pristine $Co_2/WS_2$ system, the matrix elements $\langle z^2|L_x|yz\rangle$ and $\langle yz|L_x|z^2\rangle$ make the main contribution to negative MAE due to the large $d_{yz}$ and $d_{z^2}$ states around $E_f$. As 0.1 e/unit charge is injected, the increased unoccupied minority-spin $d_{xz}$ and $d_{yz}$ states will raise the value of $\langle xz|L_z|yz\rangle$ and $\langle yz|L_z|xz\rangle$, whereas the decreased occupied minority-spin $d_{z^2}$ states will diminish the value of $\langle z^2|L_x|yz\rangle$. As a result, the MAE changes from −0.36 to 1.07 meV (seeing figure 3(d)). When the injected charge is −0.6 e/unit cell, compared with pristine $Co_2/WS_2$ system, the unoccupied minority-spin $d_{z^2}$ states greatly increase and the spin-conservation term $\langle yz|L_x|z^2\rangle$ make a considerable contribution to the charge of MAE value. Consequently, the MAE value reduces from −0.36 to −0.75 meV.

## 4. Conclusions

In summary, we design two kinds of Co-adsorbed monolayer $WS_2$ frameworks, $Co_1/WS_2$ and $Co_2/WS_2$, and systematically investigate the dependences of their magnetic properties on injected charge by using first-principles DFT calculations. TDOS suggest that the half-metallicity is generated in the two pristine systems. Their magnetic moments can be tuned almost linearly through charge injection due to the modulated interactions and charge transferring between Co atom and monolayer $WS_2$, and a transition from ferromagnetism to non-ferromagnetism occurs in $Co_1/WS_2$ system when 1 e/unit cell charge is injected. Besides, the magnetic easy axis can be changed from in-plane direction to out-of-plane direction through charge injection as well. The decomposed orbital contributions reveal that the changes of Co-3d states are responsible for the tunable magnetic anisotropy. This work provides a theoretical background on magnetism manipulation in low-dimensional system, and opens up a great prospect for the design and fabrication of 2D spintronics devices.

## Acknowledgments

This work was supported by the National Key Research and Development Program of China (Grant No. 2018YFB0406603), the National Natural Science Foundation of China (Grant No. 61974123, 61774128, 61674124, 61874092, and 61804129), the Science and Technology Project of Fujian Province of China (Grant No. 2018I0017), the Fundamental Research Funds for the Central Universities (Grant No. 20720190055), Science and Technology Key Project of Xiamen (Grant No. 3502ZCQ20191001).

## ORCID iDs

Weiqing Tang https://orcid.org/0000-0001-5355-3993
Zhiming Wu https://orcid.org/0000-0002-9642-6449
Yaping Wu https://orcid.org/0000-0001-9325-2212
Xu Li https://orcid.org/0000-0002-0377-2925

## References


[1] Khajetoorians A A, Baxevanis B, Hubner C, Schlenk T, Krause S, Wehling T O, Lounis S, Lichtenstein A, Pfannkuche D, Wiebe J and Wiesendanger R 2013 *Science* **339** 55–9

[2] Carbone C *et al* 2011 *Adv. Funct. Mater.* **21** 1212–28

[3] Qi M Y, Dai S H and Wu P 2020 *J. Phys.: Condens. Matter* **32** 085802

[4] Ma X X and Hu J 2018 *ACS Appl. Mater. Interfaces* **10** 13181–6

[5] Pal A N, Li D Z, Sarkar S, Chakrabarti S, Vilan A, Kronik L, Smogunov A and Tal O 2019 *Nat. Commun.* **10** 5565

[6] Sierda E, Elsebach M, Wiesendanger R and Bazarnik M 2019 *Nano Lett.* **19** 9013–8

[7] Yu H, Cui X, Xu X and Yao W 2015 *Natl Sci. Rev.* **2** 57–70

[8] Schaibley J R, Yu H, Clark G, Rivera P, Ross J S, Seyler K L, Yao W and Xu X 2016 *Nat. Rev. Mater.* **1** 16055

[9] Yun W S and Lee J D 2014 *Phys. Chem. Chem. Phys.* **16** 32528–33

[10] Luo M, Xu Y E and Shen Y 2017 *J. Supercond. Nov. Magnetism* **30** 2849–54

[11] Fang Q L, Zhao X M, Huang Y H, Xu K W, Min T, Chu P K and Ma F 2018 *Phys. Chem. Chem. Phys.* **20** 553–61

[12] Kanoun M B 2018 *J. Alloys Compd.* **748** 938–42

[13] Zhang W *et al* 2019 *ACS Nano* **13** 2253–61

[14] Cong W T, Tang Z, Zhao X G and Chu J H 2015 *Sci. Rep.* **5** 9361

[15] Jiang C H, Zhou R Q, Peng Z H, Zhu J F and Chen Q 2016 *Phys. Chem. Chem. Phys.* **18** 32528–33

[16] Fu M M, Tang W Q, Wu Y P, Ke C M, Guo F, Zhang C M, Yang W H, Wu Z M and Kang J Y 2018 *J. Phys. D: Appl. Phys.* **51** 205001

[17] Yang H X, Vu A D, Hallal A, Rougemaille N, Coraux J, Chen G, Schmid A K and Chshiev M 2016 *Nano Lett.* **16** 145–51

[18] Ou X D, Wang H B, Fan F R, Li Z W and Wu H 2015 *Phys. Rev. Lett.* **115** 257201

[19] Rau I G *et al* 2014 *Science* **344** 988–92

[20] Song Y X, Tong W Y, Shen Y H, Gong S J, Tang Z and Duan C G 2017 *J. Phys.: Condens. Matter* **29** 475803

[21] Wyrick J, Natterer F D, Zhao Y, Watanabe K, Taniguchi T, Cullen W G, Zhitenev N B and Stroscio J A 2016 *ACS Nano* **10** 10698–705

[22] Ren J D, Guo H M, Pan J B, Zhang Y Y, Wu X, Luo H G, Du S X, Pantelides S T and Gao H J 2014 *Nano Lett.* **14** 4011–5

[23] Liu R H, Lim W L and Urazhdin S 2015 *Phys. Rev. Lett.* **114** 137201

[24] Tudu B and Tiwari A 2017 *Vacuum* **146** 329–41

[25] Ruiz-Diaz P, Dasa T R and Stepanyuk V S 2013 *Phys. Rev. Lett.* **110** 267203

[26] Gong S J, Duan C G, Zhu Z Q and Chu J H 2012 *Appl. Phys. Lett.* **100** 122410

[27] Song C S, Gong S J, Zhang Z X, Mao H B, Zhao Q, Wang J Q and Xing H Z 2015 *J. Phys. D: Appl. Phys.* **48** 485001

[28] Perdew J P, Burke K and Ernzerhof M 1996 *Phys. Rev. Lett.* **77** 3865–8

[29] Baerends E J 2000 *Theor. Chem. Accounts* **103** 265–9

[30] Tang W Q, Ke C M, Fu M M, Wu Y P, Zhang C M, Lin W, Lu S Q, Wu Z M, Yang W H and Kang J Y 2018 *Phys. Lett.* A **382** 667–72

[31] Ke C M, Tang W Q, Zhou J P, Wu Z M, Li X, Zhang C M, Wu Y P, Yang W H and Kang J Y 2019 *Appl. Phys. Express* **12** 031002

[32] Xie Q D *et al* 2019 *Adv. Mater.* **31** 1900776

[33] Li Z R, Mi W B and Bai H L 2018 *Appl. Phys. Lett.* **113** 132401

[34] Nazir S, Jiang S C, Cheng J L and Yang K S 2019 *Appl. Phys. Lett.* **114** 072407

[35] Pan Y, Fölsch S, Lin Y-C, Jariwala B, Robinson J A, Nie Y, Cho K and Feenstra R M 2019 *2D Mater.* **6** 021001

[36] Zhu H-L, Yang W-H, Wu Y-P, Lin W, Kang J-Y and Zhou C-J 2015 *Chin. Phys.* B **24** 077301

[37] Zheng H L, Yang B S, Wang D D, Han R L, Du X B and Yan Y 2014 *Appl. Phys. Lett.* **104** 132403

[38] Qu J X and Hu J 2018 *Appl. Phys. Express* **11** 055201

[39] Cai G Z, Wu Z M, Guo F, Wu Y P, Li H, Liu Q W, Fu M M, Chen T and Kang J Y 2015 *Nanoscale Res. Lett.* **10** 126